Accident Analysis and Prevention 168 (2022) 106594

Contents lists available at ScienceDirect

Accident Analysis and Prevention

journal homepage: www.elsevier.com/locate/aap

Artificial intelligence-aided railroad trespassing detection and data analytics: Methodology and a case study

Zhipeng Zhang [a,b], Asim Zaman [b], Jinxuan Xu [c], Xiang Liu [b,*]

[a] Shanghai Key Laboratory for Digital Maintenance of Buildings and Infrastructure, School of Naval Architecture, Ocean and Civil Engineering, Shanghai Jiao Tong University, China
[b] Department of Civil and Environmental Engineering, Rutgers, The State University of New Jersey, USA
[c] Department of Electrical and Computer Engineering, Rutgers, The State University of New Jersey, USA

ARTICLE INFO

Keywords:
Trespassing
Railroad safety
Artificial Intelligence
Computer vision
Risk management

ABSTRACT

The railroad industry plays a principal role in the transportation infrastructure and economic prosperity of the United States, and safety is of the utmost importance. Trespassing is the leading cause of rail-related fatalities and there has been little progress in reducing the trespassing frequency and deaths for the past ten years in the United States. Although the widespread deployment of surveillance cameras and vast amounts of video data in the railroad industry make witnessing these events achievable, it requires enormous labor-hours to monitor real-time videos or archival video data. To address this challenge and leverage this big data, this study develops a robust Artificial Intelligence (AI)-aided framework for the automatic detection of trespassing events. This deep learning-based tool automatically detects trespassing events, differentiates types of violators, generates video clips, and documents basic information of the trespassing events into one dataset. This study aims to provide the railroad industry with state-of-the-art AI tools to harness the untapped potential of video surveillance infrastructure through the risk analysis of their data feeds in specific locations. In the case study, the AI has analyzed over 1,600 h of archival video footage and detected around 3,000 trespassing events from one grade crossing in New Jersey. The data generated from these big video data will potentially help understand human factors in railroad safety research and contribute to specific trespassing proactive safety risk management initiatives and improve the safety of the train crew, rail passengers, and road users through engineering, education, and enforcement solutions to trespassing.

1. Introduction

Based on statistics from the Federal Railroad Administration (FRA) of the United States (U.S.) Department of Transportation, the U.S. railroad system is comprised of approximately 830 railroads, 134,000 miles of track, and 210,000 railroad crossings (FRA, 2018a). Trespassing accidents along rights-of-way (ROW) and at highway-rail grade crossings constituted over 90% of rail-related deaths over the past ten years (FRA, 2018a). More specifically, there were 855 trespass-related fatalities in 2017, which demonstrated an increase of 18 percent from 2012 (FRA, 2018b). In addition to fatalities, these incidents resulted in other serious consequences, such as nonfatal injuries, train derailments, hazardous material spillage, train delays, and traffic congestion. From 2012 to 2016, trespassing accidents in the United States cost railroads and society approximately $43 billion (FRA, 2018b), a sum that did not cover indirect costs (e.g., emotional distress or productivity losses). The FRA (2016a) concluded that most trespassing deaths occurring each year are preventable if effective countermeasures were implemented.

Amongst the limited studies of railroad trespassing, most researchers encountered challenges due to limited data resources and uncertain data quality. Most publicly available trespassing data takes the form of casualty information or grade crossing accidents, and does not include near-miss events. However, the FRA (2018b) postulated that the number of trespassing occurrences each year far exceeds the number of fatalities and injuries and more data on trespassing events that do not result in casualties would be valuable to railroad safety researchers. In other words, while the accident reports submitted to the FRA by railroads have proven to be helpful to railroad researchers, most of the valuable data on trespassing is still missing. Trespassing events indicate certain behaviors that may lead to severe consequences if they occur repeatedly. Specifically, the near-miss events of trespassing, involving common causation against trespassing accidents, can contribute to developing the

* Corresponding author.

https://doi.org/10.1016/j.aap.2022.106594
Received 4 November 2021; Received in revised form 9 January 2022; Accepted 31 January 2022

perceptions of trespassing risks with a sufficient number of events. Learning from these trespassing events is critical towards better education for the public on trespassing safety, law enforcement, and engineering solutions to prevent trespassing on railroad tracks. The increasing availability of video data in the rail industry makes the collection of trespassing data more feasible.

Deployment of camera systems continues to increase in the United States following the 2015 Fixing America's Surface Transportation (FAST) Act, which mandated the installation of cameras throughout passenger rail lines to promote safety objectives (FRA, 2015). In addition, the Transportation Security Authority (TSA) provided funding for surveillance in transit and passenger rail areas (Elias et al., 2016). Cameras can be found throughout rail lines, yards, bridges, grade crossings and stations, which provide numerous video data sources for railroads. However, most camera systems are reviewed manually by railroad crew, train police, or local police which is labor-intensive and expensive. Limited resources and operator fatigue (Dee and Velastin, 2008) can potentially lead to missing trespassing events. Besides, the trespassing incident/accident risks along the right-of-ways and at grade crossings are challenging to monitor and to manage since they involved non-railroad personnel (e.g., pedestrian, vehicle drivers). To address these challenges and leverage the untapped potential of this big video data, this research develops a novel Artificial Intelligence (AI)-aided tool that is capable of localizing and identifying trespassing events in both archival video data and live streams with acceptable processing speed and accuracy. You Only Look Once (YOLO), an emerging object detection algorithm developed by Redmon et al. (2016), Redmon and Farhadi (2018), is utilized in the trespassing detection methodology to achieve high-accuracy trespassing detection with relatively low computation cost. With this practice-ready technology, over two months of video data from one grade crossing are processed and over 3,000 trespassing events are detected and analyzed in this study. These detected events, along with recorded trespassing video clips, can contribute to developing practical trespassing risk mitigation strategies and improving the safety of the train crew, rail passengers, and road users.

2. Literature review

2.1. Trespassing on railroad property

Railroad trespassing is defined as an event when any unauthorized person or vehicle enters or remains on a railroad right-of-way, grade crossing, equipment, or facility (FRA, 2018b). Railroads own their rights-of-way and have a reasonable expectation of operating on their property without the presence or interference of unauthorized persons. Pedestrians and motorists are only permitted on railroad property where a roadway intersects with the railroad tracks at the same level or grade, provided that highway traffic control signals and other signage are obeyed. Railroads have continuously struggled with the issue of trespassing at highway-rail grade crossings and the rights-of-way (ROW), which can have serious consequences, such as fatalities and injuries, train derailments, hazardous material spillages, train delays and traffic congestion.

Prior research has largely focused on evaluating common countermeasures and understanding the factors that influence trespassing. Havârneanu et al. (2015) concluded 19 main preventative measures in worldwide areas (e.g., New Zealand, Germany, US, UK, Japan, and Austria) based on a review of 139 publications from 1978 to 2014 and classified them into behavioral measures and engineering measures. The solutions to prevent trespassing accidents/incidents fall under the traditional safety concept of the 3 E's (Engineering, Enforcement, Education) (Chadwick et al., 2014). Most common classes of engineering countermeasures to date are flashing lights and gates, traffic dividers, fencing/physical barriers, and surveillance systems. The FRA works closely with law enforcement agencies across the United States to improve railroad crossing safety and trespass prevention (FRA, 2015). Furthermore, the railroad industry and Operation Lifesaver have devoted most of their efforts to educating the public in the United States and have been effective in reducing collisions at grade crossings and railroad rights-of-way (Frittelli, 2018). Education programs have also been implemented in Israel (Rosenbloom et al., 2008) and New Zealand (Lobb et al., 2003) along with railroad safety workshops and school lessons. However, these studies were limited in scope. For example, Lobb et al. (2003) studied the education-related strategy for a period of four weeks in one school and Rosenbloom et al. (2008) evaluated countermeasures based upon questionnaires given to 180 pupils. In terms of influencing factors, the occurrence of trespassing events is correlated with several organizational factors, environmental factors, personal factors, and psychological factors. Gender and age are the most widely studied correlation factors. Compared to females and seniors, most fatalities from trespassing are young males, who lack awareness of potential dangers (Lobb et al., 2003; George, 2008). Regarding age, a prior study (George, 2008) concluded that two out of every three railroad trespassing fatalities occurred between the ages of 20 and 49 and the reported fatalities' mean age at time of death was 37.9 years. This trend changes across the globe, for example, in New Zealand the average age of victims was between 10 and 19 years (Lobb et al., 2003). Other factors were also mapped, such as the use of alcohol and/or drugs (George, 2008; Silla and Luoma, 2012) and weather conditions (Savage, 2016).

To the authors' knowledge, most trespass-related studies typically used publicly accessible accident data, as well as demographic and economic data. However, Stanchak and DaSilva (2014) concluded that much of the academic literature on trespassing risk is inconclusive due to limited data and uncertain data quality. The trespassing accident data represents a limited proportion of all trespassing events, the greater remainder being trespass incidents that are defined as near-miss events. Near misses have several features, such as common causation against accidents (Wright and Van der Schaaf, 2004) and occur repeatedly, which allows for significant statistical analyses. Near misses, as frequent events having impacts on the perceptions of risk, have been employed in the studies of transport and recreational cyclists (Poulos et al., 2017) and the fire and emergency services industry (Taylor et al., 2014). Thus, there is a definite need for research analyzing near-miss events to determine how to mitigate highway-rail grade crossing and right-of-way risks more efficiently. However, there are fewer publications focused on near-miss events due to the lack of near-miss data and the lack of a data collection methodology. There are only four near miss-involved research initiatives (Fig. 1), which are limited in scope due to considerable costs of data collection. To overcome this limitation, a generic methodology aiming to collect trespassing events (including near misses) and reinforce trespassing risk reduction is proposed in this paper.

2.2. Railroad trespassing detection technologies and methodologies

Previous studies have employed various technologies to detect trespassing over railroad infrastructure in the past decade. DaSilva et al. (2012) demonstrated an automated prototype railroad infrastructure security system installed at a bridge in Pittsford, New York. This location was selected due to numerous accounts of trespassing and fatalities. The key component of this system is the dual-technology motion detector that combines stereo Doppler microwave technology with a passive infrared sensor. Although this motion sensor can be activated by an approaching trespasser, the system still needed attendants to observe videos from installed camera and determine whether there is a trespasser. A similar trespass detection sensor was also developed and installed in Brunswick, Maine (Volpe Center, 2015). However, these technologies are based on the conglomeration of several devices which makes them susceptible to component failure, resulting in downtime (DaSilva et al., 2012).

In one recent study of an overpass bridge going over a grade crossing (Ngamdung, 2019), the overpass utilization was collected using an

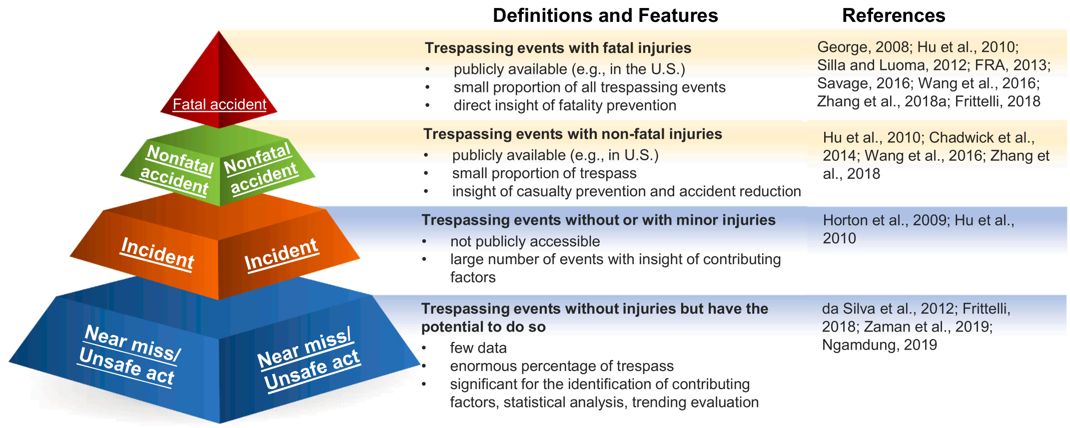

Fig. 1. Pyramid Chart for Trespassing Events in Fatal Accident, Nonfatal Accident, Incident, and Near Miss.

automated pedestrian counter, while the pedestrian trespass under the bridge was manually coded based on video data. However, the manual counting of trespassing events for 100 h of video is expected to have considerable labor costs. Meanwhile, in one recent study on railroad trespassing, Topel (2019) concluded that the manual detection from surveillance is labor-intensive and expensive, and instead suggested automated detection as one way to potentially reduce the need for human monitors. To detect and collect trespassing events in an efficient, reliable way, an Artificial Intelligence-based trespassing detection methodology is proposed in this paper to detect trespassing events from large amounts of video data. For example, Zhang et al. (2018b) identified and tracked the trespassing events with background subtraction and the moving pixels of objects. In the daytime, a moving-object binary mask was constructed with background subtraction in each frame and binary thresholding. During the nighttime, the proposed method developed a different process since light makes objects brighter and increases the object's pixel intensity.

2.3. *Artificial Intelligence with computer vision*

The implementation of Artificial Intelligence (AI) in computer vision has the potential to greatly reduce the required manpower to detect objects from video data. Evidence of this exists within the utilization of AI algorithms in parallel industries, such as highway (Arabi et al., 2020), sidewalk (Yencha, 2019), and aviation (Qu et al., 2017). Deep learning models in AI can be used in the domain of automatic maintenance of transportation and civil infrastructure to significantly reduce human intervention and operational costs.

In the AI-based object detection, there are two major groups of algorithms, region-based object detectors and single shot detectors. All these AI-based object detection algorithms employ the well-established architecture of Convolutional Neural Networks (CNN). The major difference between these two groups is the way to process images and detect objects. In the region-based family, potential bounding boxes in an image are first generated with region proposal methods, such as Region Proposal Network (RPN) with developed classifier. With classification, these extracted bounding boxes are refined with post-processing and duplicate detections are eliminated (Girshick et al., 2014). However, the complex pipelines in region-based CNN methods are slow and difficult to optimize because each individual component must be trained separately (Redmon et al., 2016). Instead, in single shot methods (e.g., YOLO), a single CNN is used to predict bounding box coordinates and class probabilities (Redmon et al., 2016). Therefore, single shot detection algorithms tend to run faster than region-based algorithms that have a relatively more complex pipeline. Detailed comparison between region-based object detectors and single shot detectors can be found in Li et al. (2020). Table 1 demonstrates the previous studies in trespassing detection with region-based object detectors, complex detector-based systems, and manual monitoring.

Table 1
Previous studies in trespassing detection.

Reference	Application	Methodology	Limitation
DaSilva et al., 2012	Right-of-way trespassing detection in Pittsford, New York	An automated prototype security system combining stereo Doppler microwave technology (motion detection), a dual element passive infrared sensor (heat detection), and camera	• Reliability became one major concern in the complex system • False alarm rate remained a particular problem
Volpe Center, 2015	Right-of-way trespassing detection in Brunswick, Maine		
Catalano et al., 2014	No real-world application	An integrated optical fiber system composed of Fiber Bragg Gratings (FBG) strain sensors	• Detect human walking only and not test with different moving targets • Subject to false positive from interfering events • Reliability was one major concern in the complex system
Ngamdung, 2019	Right-of-way trespassing detection in Collegeville, Alabama	Camera and manual detection	• Labor-intensive and expensive
Zhang et al., 2018b	Highway-rail grade crossing trespassing detection in New Jersey	Camera and computer vision methodologies (e.g., background subtraction, image segmentation, and Kalman Filtering)	• Requires extensive reconfiguration for new applications • Limited object recognition • Only 2-day data in validation and application
Zaman et al., 2019	Both Highway-rail grade crossing and right-of-way trespassing detection in Ashland, Virginia and Thomasville, North Carolina	Camera and deep learning method called Mask R-CNN	• Very high computational cost • Slow archival review speed • Limited data in validation and application

YOLO is an emerging state-of-the-art object detection algorithm that is faster than most other popular object detection frameworks but maintains high accuracy. It has been successfully used in analyzing big video data from several transportation domains, such as traffic congestion detection (Chakraborty et al., 2018), license plate recognition (Laroca et al., 2018), and traffic signs (Zhang et al., 2017), with high accuracy and fast processing speed. In this paper, YOLO is employed as the key AI algorithm in the automatic detection of trespassing events from video data of highway-rail grade crossings and rights-of-way.

Overall, the widespread usage of surveillance cameras and corresponding video data provide opportunities to study near-miss events. The AI algorithm, such as YOLOv3, makes detecting these trespassing events achievable in a manner of high efficiency. There is a need for a robust, AI-based automatic trespassing event detection framework that can be adapted to grade crossings and rights-of-way throughout the railroad system to support railroad safety decisions and ultimately save lives.

3. Methodology

3.1. Overview of You Only Look Once (YOLO)

YOLO uses features learned by a single deep convolutional neural network to detect objects. As introduced in the previous section, most deep learning-based object detection algorithms, such as the R-CNN family, have a complex detection pipeline, in which bounding box generation, object classification, duplicate detection elimination, and bounding box refining and rescoring are executed sequentially. Instead, YOLO sees the entire image or video frame and implicitly encodes contextual information about classes as well as their appearance (Redmon et al., 2016). In this algorithm, object detection is redefined as a regression problem to spatially separate bounding boxes and associated class probabilities with one single Convolutional Neural Network. The generic architecture of YOLO and R-CNN are presented in Fig. 2.

YOLO's performing as a single-stage detector can be faster than other deep learning-based methods and meets the need for real-time processing with limited computational resources. In this paper, YOLO indicates YOLOv3 particularly, which is the third generation and the most recent object detection algorithm in YOLO family. Overall, YOLO is expected to achieve the necessity of real-time object detection, as well as archival videos, with stable accuracy that are key requirements in the trespassing detection of this study.

3.2. YOLO-Based trespassing detection framework

There are five major phases in trespassing detection with YOLO and computer vision: video frame input, region of interest (ROI) designation, YOLO-based object detection, object tracking, and output collection and follow-up actions. Fig. 3 presents a systematic illustration of this detection technology. The developed detection tool can be applied to two safety–critical scenarios: rights-of-way and highway-rail grade crossings.

- Railroad right-of-way is defined as the railroad property with no intersection or crossing. For trespassing along rights-of-way, any unauthorized movements of people or vehicles within the rights-of-way would be deemed illegal at any moment and identified as trespass violations.
- A highway-rail grade crossing is the intersection between the highway and railway, where active signalizations are commonly installed to alert highway users to an approaching train. Trespassing at a highway-rail grade crossing is defined as when pedestrians and vehicles enter the crossing zone while the signal lights are activated, though the highway users' behaviors in other cases would be permissible.

3.2.1. Video input preparations

The first step of the developed AI framework is to import either live video streams or archival video data. Frames are extracted from videos and processed as the input image in the AI framework. Instead of reading every frame within a video, the algorithm should be tuned to achieve an optimal trade-off between processing speed and accuracy. To be processed in real time or an even shorter time, the number of frames per second in tuned videos should be smaller than the number of frames/images that the graphics processing unit (GPU) is able to process in one second. Accuracy should be maintained with a sufficient number of frames.

3.2.2. Designation of region of interest

The region of interest (ROI) is defined as the area that pedestrians and highway users are prohibited from entering. To designate the ROI in trespassing cases, a user can sequentially select the outer limits of the trespass area in the static image of the video. Since this study focuses on videos from fixed cameras only, one pre-defined ROI, as an enclosed polygon, is practical for all image processing in one location.

3.2.3. YOLO-based trespass detection

Along rights-of-way, any unauthorized pedestrian or vehicle detected in the ROI are deemed to be trespassing. The highway-rail grade crossing will only trigger trespass event detection if the signal lights and crossing gates are activated. This categorization represents the two fundamentally different types of locations where trespassing occurs. Both scenarios are analyzed by the same generalized trespass detection framework, except for the trigger of signal light serving as the preceding condition in highway-rail grade crossings.

3.2.3.1. Activated signal light detection. In highway-rail grade crossing trespass detection, one precondition is the identification of activated red signals. From the computer vision perspective, the identification of a red signal can be achieved with red pixel values in one small zone where the red signals are located. Zhang et al. (2018b) provided a red signal

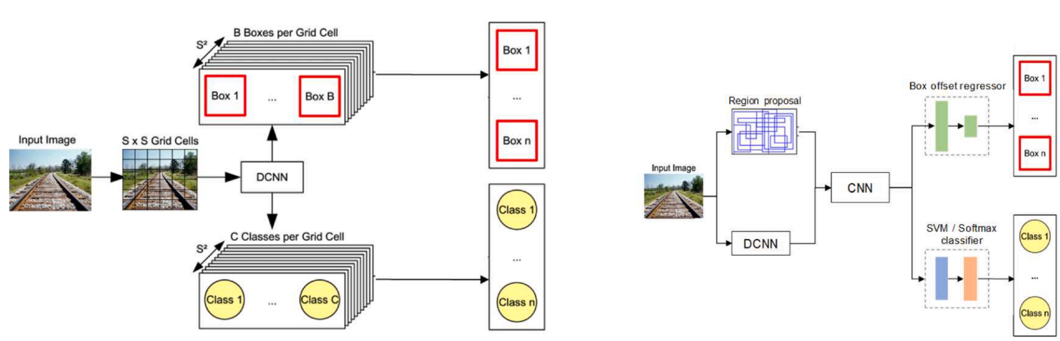

(a) YOLO (b) R-CNN

Fig. 2. Architectures for Object Detection in (a) YOLO and (b) R-CNN. Notes: In R-CNN, DCNN is for pre-training and CNN is fine-tuned for region features.

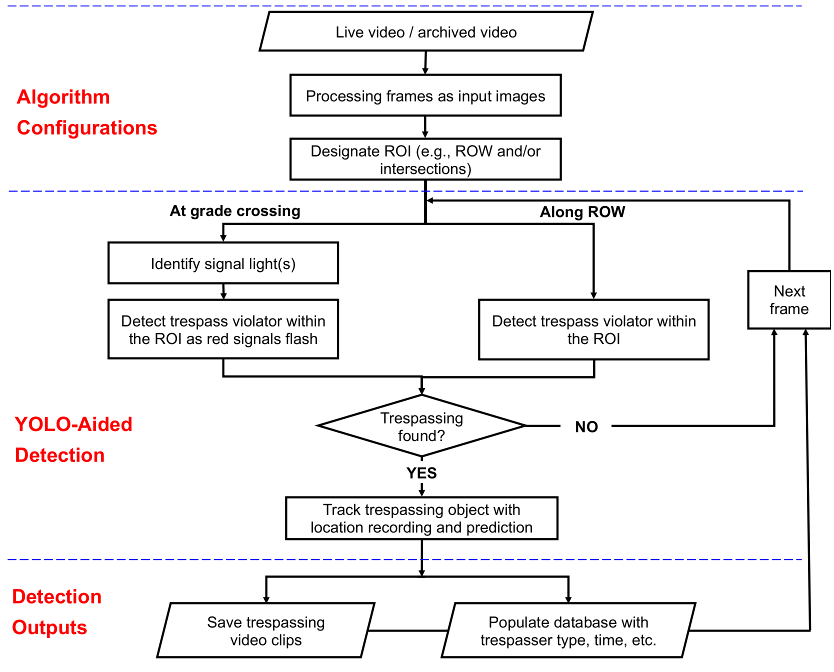

Fig. 3. General YOLO-Based AI Framework for Railroad Trespass Detection.

indication method, in which the intensity difference of two lamps emitting red lights in the stop signal was the reference for stop signal detection. More specifically, two small square windows in RGB (red, green, blue) color scale are extracted from the left signal lamp and the right signal lamp respectively (Fig. 4). The equation below is used to convert two signal lamps' RGB into grayscale:

$$\Phi(x_{RGB}) = x_{GRAY} = (0.2989) \times x_R + (0.5870) \times x_G + (0.1140) \times x_B \tag{1}$$

where x_R, x_G, x_B, x_{GRAY} are color values for red, green, blue, and gray respectively.

Based on this transformation, the gray scale representations of left signal window (L_{GREY}) and right signal window (R_{GREY}), as well as the absolute intensity difference δ, can be calculated,

$$L_{GREY} = (\Phi_L(x_{RGB})) \in [0, 1]^{n\times n} \tag{2}$$

$$R_{GREY} = (\Phi_R(x_{RGB})) \in [0, 1]^{n\times n} \tag{3}$$

$$\delta = |Q_2(L_{GREY}) - Q_2(R_{GREY})| \tag{4}$$

where n is the size of signal lamp window; function Q_2 is the 50%

Fig. 4. Intensity Difference of Stop Signal During Day and Night (Zhang et al., 2018b).

quantile in signal window.

If the absolute intensity difference δ between the two lamps is greater than a threshold (α), the status of the signal light is identified as "on", while correspondingly the status is identified as being "off" if the absolute intensity difference δ being smaller than the threshold. The threshold α of color difference can be configured based upon training video data. Previous studies (Zhang et al., 2018b; Zaman et al., 2019) have proven that this method is feasible in the testing of trespassing detection algorithms for both daytime and nighttime conditions.

3.2.3.2. YOLO-aided object detection. With pre-defined ROI and red signal identification, the YOLO-based algorithm can analyze frames of the live video feed or archival video data. A key part of YOLO performance is the training dataset which allows it to recognize objects. This study uses COCO, a large-scale object detection dataset, for the training data. The COCO dataset includes over 330,000 images, more than 200,000 labeled images, and 80 object categories. Due to its depth, diversity, and continuous growth and refinement, COCO dataset has been employed in object recognition research and gives computer vision algorithms valuable training data to recognize commonly seen objects (Lin et al., 2014). These features coupled with YOLO allow for rapid deployment of AI in object recognition tasks.

As shown in the conceptual diagram of trespassing detection (Fig. 5), the YOLO network is fed with input images/video frames and outputs with bounding box coordinates and objectness scores. The dimension of an output tensor is:

$$S \times S \times [B \times (5 + C)] \quad (5)$$

Where: $S \times S$ is the scale of input images; B is the number of boxes that each grid predicts; 5 is the box coordinates (tx, ty, tw, th) and objectness score (the level of certainty); and C is the number of classes (e.g., person, car, truck).

In general, to execute a detection, the image (a certain frame from the video stream) is divided into a grid of $S \times S$ (left image). Each one of the S^2 cells will predict B possible bounding boxes and the objectness score (the level of certainty) of each of them, such that $S \times S \times B$ boxes are generated and calculated. Most of these boxes will have a very low probability, which is the reason why the algorithm proceeds to delete the boxes that are below a certain minimum threshold of minimum probability. The remaining boxes are passed through a non-max suppression, which eliminates possible duplicate objects (Fig. 5).

3.2.4. Object tracking

A limitation of the YOLO network is that it cannot inherently remember and track objects from frame to frame. Detection results from the YOLO network can only provide the detected object information from each individual image (frame). It is a challenge to distinguish these "new" objects from the "old" objects that also exist in the previous frames, which comprises the huge discrepancy between image processing and video analysis. The distinct consequence of erroneous categorization is that the number of trespassing occurrences increases rapidly due to recurrent counting of objects in frames. Therefore, the proper categorization of detected objects is crucial to ensure detection accuracy in trespassing video analysis.

Object tracking is based on the position of objects. The position of each object in one frame is recorded and a mask window including all possible positions where objects may appear in the next frame is predicted using a Kalman Filter (Kalman, 1960). In the next frame, if there is an object detected in the predicted area from the last frame, these two detected objects are identified as the same object. This process is repeated for each analyzed frame of video to maintain continuous object tracking. If the predicted location is out of ROI, it means that this object has already left the ROI or the image. Consequently, we can stop tracking it and then generate output for this detected object.

3.2.5. Output

If an illegal object is detected within the ROI, a subroutine of the AI will execute the commands with several outputs (Fig. 5). A clip of the

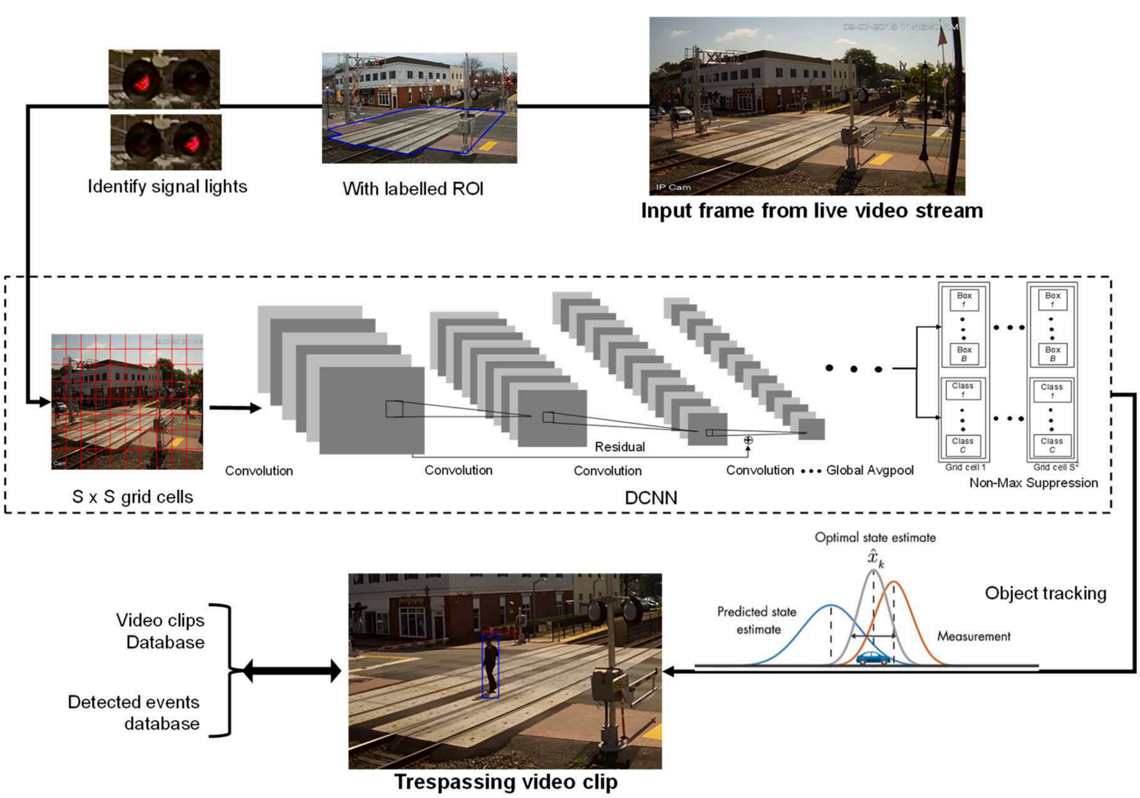

Fig. 5. Conceptual Trespassing Detection System Using Artificial Intelligence.

trespass event is recorded and metadata (e.g., trespassing type, time, video file name etc.) is stored in a trespass event database. This metadata is automatically generated by the AI, demonstrating that the context of the image can be extracted and interpreted. Trespass data can provide valuable information about hazardous environments and trespassing behaviors that can inform education, enforcement, and engineering strategies for trespass prevention. Additionally, the aggregation of these trespass events has the potential to enhance future railroad risk analyses.

Furthermore, in the implementation of AI-based trespassing detection technology, combining computer vision techniques and the YOLO algorithm, detection accuracy can be increased through configuration and testing. Additional datasets, including diverse environmental conditions (e.g., rain, snow, day, night and fog) and distortions (e.g., video artifacts, shadows) should be tested to verify its performance under varying circumstances.

4. Case study - Algorithm implementation in one grade crossing

4.1. Overview of selected grade crossing

To validate the functionality of the proposed AI-based trespassing detection technique, a grade crossing located in New Jersey is selected as a case study, although the developed methodology can also be applied to rights-of-way. The selected crossing experiences about 110 activations per day, with the majority being commuter trains. One train station with three parking lots, two to the west of the train tracks and one to the east, are adjacent to the grade crossing. Several restaurants, markets, and two schools are located along the busy downtown street (Fig. 6).

Trespassing in the selected grade crossing is reportedly commonplace and fatalities have occurred in the past decade (FRA, 2019a). Per the FRA Form 6180.57 (FRA, 2019b), at least four fatal grade crossing accidents have occurred at the selected grade crossing since 2010. Per observations from videos and field visits, grade crossing trespasses occur there every day.

Most violations do not involve damage or injuries and accidents are (fortunately) too few to provide a significant statistical sample to support decision making about investing in safety improvements. However, the few accidents that have occurred were preceded by trespassing, and gathering data on near misses will dramatically increase the data available to formulate solutions to this problem. This lack of data is the prime motivation for the AI-aided trespassing detection methodology developed in this research.

4.2. AI-Aided detection technology configuration and processing

4.2.1. Video data preparation

During the data collection, one IP camera is mounted on a utility pole located approximately 30 feet northwest of the grade crossing, as shown in Fig. 7. The camera's view can cover all activities in the grade crossing, as well as at least 5 feet on either side of this location.

In this case study, 1,632 h (68-days) of raw video data is processed to support the AI-aided methodology validation, data collection, and trespassing risk analysis. These videos continuously monitor this location with 24 h each day. The video data is in MP4 format with 30 frames per second and a resolution of 1920 pixels by 1080 pixels. With limited data availability, three time periods are studied to cover diverse seasonal conditions. Both volume and variety of studied data are significantly greater than previous research (Zhang et al., 2018a; Zaman et al., 2019). The periods are as follows:

- o April 19–25, 2018 (7 days)
- o September 2018 (30 days)
- o January 2019 (31 days)

4.2.2. ROI and red signal

In the grade crossing case study, only pedestrians and vehicles that entered the ROI after the signal is activated would trigger the detection of trespassing events. The selected grade crossing employs proactive, advanced grade crossing systems, in which flashing red lights and gates are equipped to warn and block highway users. As shown in Fig. 8, ROI in the crossing is represented by the polygon with blue lines. The right-of-way around the grade crossing is excluded in this case study due to an explicit focus on grade crossing risk. In this 1920 × 1080 video frame, the borders of ROI can be drawn through connecting a series of endpoints.

The on/off state of the stop signal is derived by focusing on the stop signal post. The stop signal consists of a left lamp and a right lamp with a size of 3 × 3 pixels emitting red light (Fig. 8). The on/off state of the red signal is identified based on the error of two median values of the lamps' gray color values. Accounting for both daytime and nighttime conditions, the intensity difference threshold of α has been fixed at 0.3 after trial and error.

4.2.3. YOLO algorithm configuration

The computing device, NVIDIA Jetson TX2 developer kit, can process one video frame in 0.45 s. The video frame reading rate is tuned to 2 frames per second to achieve a non-later than real time processing ability. Also, channels are set to 3, which indicates that this model

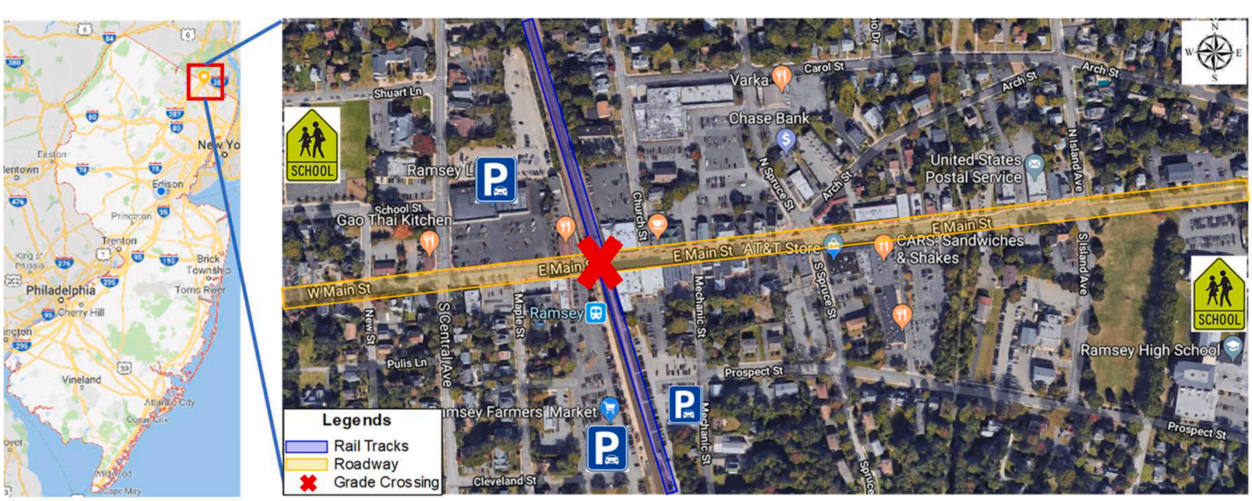

Fig. 6. Aerial View of Selected Grade Crossing.

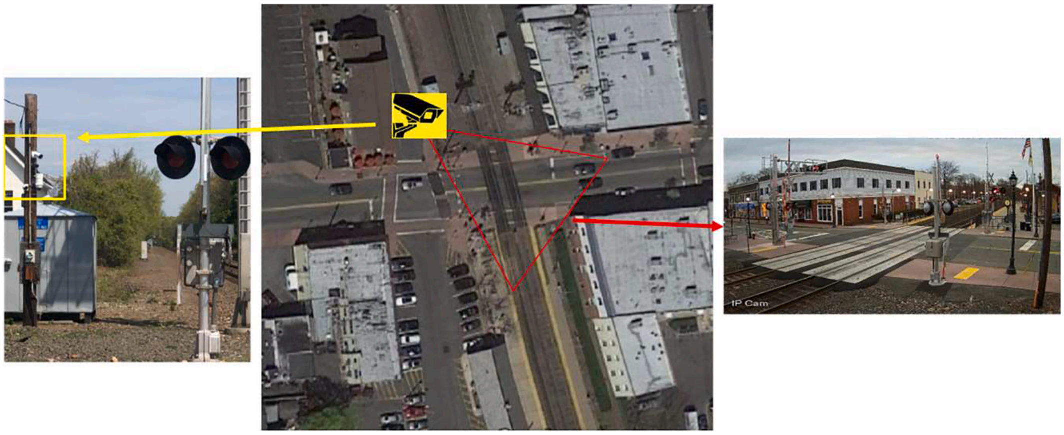

Fig. 7. IP Camera Placement at Selected Location.

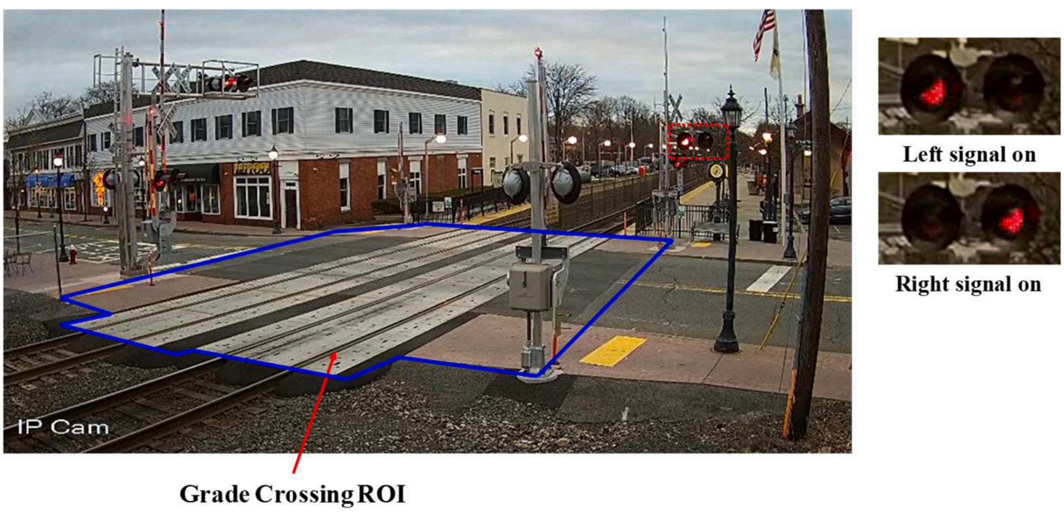

Fig. 8. Assignment of ROIs and Identification of Red Signals in Grade Crossing. (For interpretation of the references to color in this figure legend, the reader is referred to the web version of this article.)

processes 3-channel RGB input images. The batch parameter indicates the batch size used during training and testing. In this case study, the training batch size is 64 and the test batch size is 1. This means that 64 images are used in one iteration to update the parameters of the neural network and test only uses 1 image. This research uses 0.001 as the learning rate. Regarding COCO classification, there are total 80 classes in the COCO dataset. This research concentrates on 6 of them: 'person', 'bicycle', 'car', 'motorbike', 'bus', and 'truck'.

4.3. *Trespassing data collection and algorithm validation*

4.3.1. *Trespassing data collection and preparation*

In the raw video data covering two months and one week, over three thousand trespassing events are detected, and corresponding video clips are documented. The basic information pertaining to these collected trespasses, such as date and time, or the classifiers of trespassing violators (e.g., pedestrian, car, truck, bus), are recorded automatically by the AI tool. Several fields, such as daylight period and weather conditions, can be imported from publicly available data sources (e.g., https://weather.com), and traffic volumes in terms of vehicles and pedestrians can also be recorded using a computer vision-based algorithm and raw videos. Further, additional information (e.g., violator gender, gate angle, use of cell phone or headphone) regarding trespassing events may be essential. To automatically detect these features, a combination of high-resolution/frame rate cameras and more sophisticated and computationally complex deep learning AI is required. However, on average, around 35 trespassing events are documented in one-day's raw video and manually watching it only took about 6 min ($=350\mathit{seconds} = 35\mathit{clips} \times 10\mathit{secondsperclip}$), which is only 0.4% of the one-day raw video duration (1,440 min). Therefore, the developed AI-aided tool can perform as a decision support tool and the generated video clips can contribute to additional information with an efficient usage of railroad resources. Future research can focus on developing advanced functions to record these additional fields in a cost-effective way.

4.3.2. *Algorithm validation*

In this study, in addition to the raw video data, a grade crossing data supplier manually watched the same video segments from April as the developed system and recorded 407 trespassing events. This data is used to validate the accuracy of AI-aided trespassing detection tool.

In the AI-based algorithm outputs, 422 trespassing clips are originally detected. After manual review, 407 of these are validated as true trespasses and 15 are false trespasses. This means that all trespasses manually collected were detected by the developed AI algorithm without any missed detections, while several false detections were generated. Sensitivity and precision are common for computer vision detection in the literature (Le et al., 2016) and are employed to evaluate algorithm developed in this paper. Sensitivity, measured by the proportion of actual positives that are correctly identified, is 100% ($=\frac{407}{407}$)

and the precision is 96.4% ($=\frac{407}{407+15}$). Through watching trespassing clips from April, September, and January, some potential reasons behind false positives are extreme weather conditions and sunlight reflecting on the surface of red signal (Fig. 9a). Ongoing work would focus on the mitigation of noise from red signals and camera via hardware actions and algorithm enforcement.

4.4. Trespassing data analysis

4.4.1. Exploratory data analysis overview

With the implementation of the AI-aided algorithm, 3,004 positive trespassing events were captured and recorded in current database from two-months-and-one-weeks' worth of raw video data. A detailed summary of the trespassing database is presented in Table 3. On average, there were 158 trespassing pedestrians and 74 trespassing vehicles per day in the study period. In terms of solely the collected traffic volumes, the traffic counts of vehicles have similar values (around 25,000 per week) for the three time periods selected.

Based upon the number of trespasses (e.g., frequency, pedestrians, and vehicles) per day between different months, April and September 2018 have more frequent daily trespassing events and greater numbers of daily trespass pedestrians and vehicles than January 2019. For example, comparing to September 2018, the number of trespass pedestrians per day and the number of trespass vehicles per day decrease 28% ($=\frac{129-180}{180}$) and 33% ($=\frac{59-88}{88}$) in January 2019, respectively. One potential reason is that winter is expected to involve fewer outdoor activities. In the previous trespassing accident study, Savage (2016) similarly observed that fewer trespassing accidents occurred during winter months. Another potential justification for the majority declining trend in the number of trespass vehicles is a safety action taken by the New Jersey Department of Transportation (NJDOT). In November 2018, the anti-gridlock box design, a road marking stating DO NOT BLOCK was painted at the intersection between the highway and roadway. This is consistent with the results showing that the number of trespass vehicles

(a)

(b)

Fig. 9. Detection Examples (a) False Detection Extreme Due to Noises from Sunlight; (b) True Detection.

per 1,000 vehicle traffic counts in January (19) is significantly smaller than that in April (23) or September (25), as represented in Table 2.

4.4.1.1. Incidents distribution by daylight period. Assuming a 24-hour cycle, most trespass events occurred during the daytime (62.3%). In particular, the percentage of trespassing events during the daytime are over 75% for both April and September. However, January data shows close trespassing frequency in daytime, as compared to nighttime. These results are related to daylight period lengths and traffic volume in different seasons. Based upon the daylight periods and night periods of these months in selected location, daylight lengths in April and September are around 13 h, which is over one-and-a-half times the length of night periods in these two months (around 8 h). However, January has longer night period (11.20 h) than daylight period (9.55 h). Regarding traffic volume, around 74% of vehicles travelled through this grade crossing during daylight period, while night periods accounted for only 15% of vehicles for April and September combined. However, in January, only around half of vehicle traffic occurred during daylight periods and nights involved 30% of traffic volume. More detailed distributions are demonstrated in the following sections and heat maps.

4.4.1.2. Distribution by Before/After Train Pass and Gate Angle. Table 3 shows that 68.9% of trespassing events at this grade crossing occurred after the train passed through the grade crossing, whereas only 31.1% of trespassing events occurred before the train arrived. Fig. 10 shows a categorical breakdown of when trespasses occurred. The different categories are the gate position and whether the events occurred before or after the train crossed. The data supposes that trespassers are in a rush to cross the tracks after the train passes, as most of the events occurred after a train had passed and when the gate arms are between 31 and 89 degrees. A prior study revealed that 50% of respondents believed it was safe to trespass (Silla and Luoma, 2012). This could indicate that people who trespass in selected location may have a false sense of security, assuming that it is safe to trespass after the train passes. However, the selected grade crossing has multiple tracks and several videos show a second train coming on the adjacent tracks right after the first one. Furthermore, 38 trespassers exhibited dangerous behavior by crossing as the gate was closed before the train arrived and 179 trespassers violated with fully closed gates after one train passes. This population is particularly worrisome since they are the most probable trespassers to be struck by a train. Overall, the data shows that the main problem is most people trespass after the train passes. To ensure their own safety, trespassing violators should wait until the gates are fully open. This can also serve as one potential education material in the safety improvement in New Jersey and other areas.

4.4.1.3. Incidents Distribution by Gender. Out of 10,743 trespass pedestrians, 7,486 (69.7%) of them are deemed male, while only 30.3% of trespass pedestrians are female, per manual identification. Similar conclusions were also drawn in previous studies. In the investigations of trespasses, George (2008) and Silla and Luoma (2012) pointed out that most railroad-trespasser accident fatalities are males.

Meanwhile, the distribution of men and women walking through this grade crossing is also potentially one key factor. Currently there is no data on the gender distribution of grade crossing use and the collection of this data was not covered in this study. However, the population distribution by gender in this county is publicly available and the data shows that there are more women than men in the county where this grade crossing resides. Based on the statistics from the U.S. Census Bureau (2019), this county has 452,201 males (48%) and 481,371 females (52%). Overall, men are more than twice as likely to trespass at this grade crossing as female pedestrians in general, while no clear evidence supports that gender difference significantly contributes to skewing the results towards more men trespassing (Fig. 11).

Table 2
Summary of trespassing events in two months and one week.

	April 19–25, 2018		September 2018		Janaury, 2019		Sum	
	Count	Percentage	Count	Percentage	Count	Percentage	Count	Percentage
Total Number of Trespassing	407	100%	1,614	100%	983	100%	3,004	100%
Number of Trespassing per Day	58		54		32		44	
By Daylight (Total Number)								
Dark	35	8.5%	121	7.5%	443	45.1%	602	18.0%
Dawn	25	6.2%	95	5.9%	30	3.0%	152	4.6%
Day	309	75.8%	1,317	81.6%	423	43.1%	2,077	62.3%
Dusk	39	9.5%	81	5.0%	87	8.8%	210	6.3%
By Train Occurrence (Total Number)								
Before Train Passing	125	30.6%	455	28.2%	353	36.0%	944	31.1%
After Train Passing	282	69.4%	1,159	71.8%	629	64.0%	2,097	68.9%
Total Number of Trespass Pedestrians	1,342	100%	5,404	100%	3,997	100%	10,743	100%
Number of Trespass Pedestrians per Day	192		180		129		158	
By Gender (Total Number)								
Female	450	33.5%	1,640	30.4%	1,167	29.2%	3,257	30.3%
Male	892	66.5%	3,764	69.6%	2,831	70.8%	7,486	69.7%
Total Number of Trespass Vehicles	577	100%	2,634	100%	1,822	100%	5,033	100%
Number of Trespass Vehicles per Day	82		88		59		74	
Number of Trespass Vehicles per 1,000 Vehicles	23		25		19		22	
By Vehicle Type (Total Number)								
Car	511	88.7%	2,289	86.9%	1,691	92.8%	4,491	81.8%
Bicycle	65	11.3%	285	10.8%	84	4.6%	434	7.9%
Truck	0	0.0%	42	1.6%	42	2.3%	84	1.5%
Bus	0	0.0%	14	0.5%	3	0.2%	17	0.3%
Motorcycle	0	0.0%	6	0.2%	2	0.1%	8	0.1%
Total Traffic Count of Vehicles	25,233		105,811		95,676		226,720	

Table 3
Descriptive statistics of variables measured in one-hour period.

Field Name	Description	Mean	Min	25% Quantile	50% Quantile	75% Quantile	Max
Trespass_Freq	Number of trespassing events in one hour	1.9	0	0	1	2	27
Trespass_Ped	Number of pedestrian violators in one hour	4.4	0	0	1	5	82
Trespass_Veh	Number of vehicle violators in one hour	3.1	0	0	0	4	32
Veh_Traffic	Number of vehicles traveling through grade crossing in one hour (e.g., car, truck, bus, motorcycle, etc.)	191.0	0	41	151	190	1,381
After_to_Before	Percentage of trespasses occurring after train passing (0 = trespasser passed before train arrival, 1 = trespasser passed after train arrival)	0.7	0	0.5	0.8	1	1
Train_Freq	Number of passing trains in one hour	3.0	0	2	3	4	7
Weather	Clear = 1,455	–	0	0	0	1	1
	Cloudy = 1,291	–	0	0	0	1	1
	Fog = 11	–	0	0	0	0	1
	Rain = 238	–	0	0	0	0	1
	Snow = 8	–	0	0	0	0	1
Daylight_Period	Dark = 590	–	0	0	1	1	1
	Dawn = 149	–	0	0	0	0	1
	Day = 2,059	–	0	0	0	0	1
	Dusk = 206	–	0	0	0	0	1

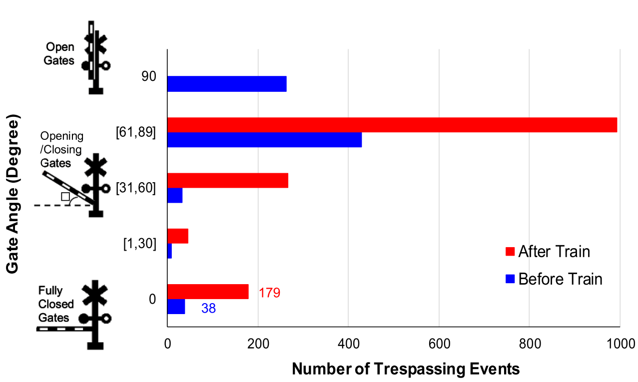

Fig. 10. Distribution of Trespassing Events by Before/After Train Pass and Gate Angle.

4.4.1.4. Incidents Distribution by Vehicle Type. The distribution of trespass vehicles shows that cars are the most common vehicle type, accounting for nearly 82% of all trespassing vehicles. Bicycles are the second largest trespassing vehicle type in the recorded trespassing events. Although only 17 buses are detected and recorded in grade crossing violations, each trespassing bus represents significant risk, particularly school buses providing services for three schools located around this grade crossing.

4.4.2. Distribution by time of the day and day of the week

4.4.2.1. Frequencies of Trespass, trespass Pedestrian, and trespass vehicle. An in-depth analysis on the distributions of trespasses by the time of the day and the day of the week was conducted. Three heatmaps in Fig. 12 show a breakdown of the number of trespassing events, number of trespassing pedestrians, and number of trespassing vehicles in a one-hour interval, respectively. Three main findings are concluded below:

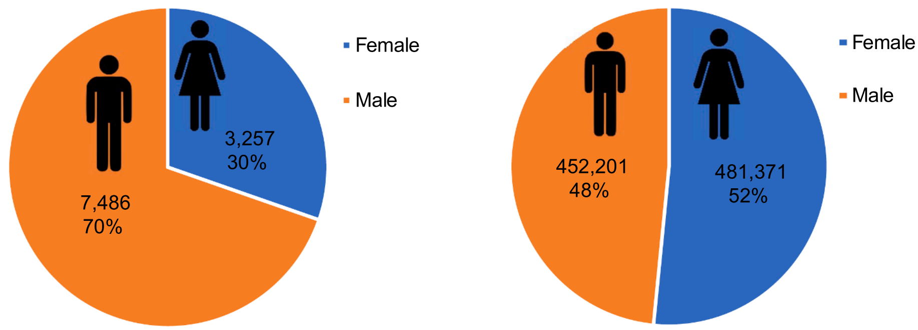

(a) Trespassers (b) Local County Population

Fig. 11. Distribution of Male vs. Female in (a) Trespassers; and (b) Local County (U.S. Census Bureau, 2019).

Day/Time	0:00	1:00	2:00	3:00	4:00	5:00	6:00	7:00	8:00	9:00	10:00	11:00	12:00	13:00	14:00	15:00	16:00	17:00	18:00	19:00	20:00	21:00	22:00	23:00	Sum
Monday	2	1	2	0	0	1	1	3	16	9	15	8	24	25	37	7	16	11	9	3	6	2	9	3	207
Tuesday	1	1	0	0	0	5	8	30	22	14	26	25	34	30	31	52	42	47	19	22	28	9	5	6	454
Wednesday	3	7	1	0	2	1	11	25	30	18	31	17	31	30	31	43	36	55	35	18	24	14	9	7	475
Thursday	5	5	0	0	2	5	15	28	26	19	18	23	19	31	27	44	34	74	48	20	23	18	10	10	501
Friday	1	6	1	0	1	0	19	31	25	23	23	24	20	31	19	40	16	63	35	22	26	9	0	11	442
Saturday	3	12	6	2	2	1	9	32	42	26	19	33	37	36	22	55	53	100	49	51	19	10	6	5	628
Sunday	3	2	1	0	0	0	2	10	22	10	32	12	27	19	47	7	31	10	28	5	10	1	11	9	296
Sum	18	34	11	2	7	13	64	157	182	118	162	140	190	199	212	250	227	361	222	140	134	62	49	50	3004

(a) Trespassing Events

Day/Time	0:00	1:00	2:00	3:00	4:00	5:00	6:00	7:00	8:00	9:00	10:00	11:00	12:00	13:00	14:00	15:00	16:00	17:00	18:00	19:00	20:00	21:00	22:00	23:00	Sum
Monday	6	3	4	0	0	1	1	25	34	31	67	25	82	104	108	7	71	34	13	15	13	1	25	10	684
Tuesday	1	1	0	0	0	10	19	92	52	22	43	55	61	65	95	111	76	209	153	160	104	36	21	12	1398
Wednesday	6	13	1	0	0	3	21	98	76	49	70	33	47	46	96	116	85	310	283	110	110	49	21	15	1656
Thursday	4	7	0	0	6	7	30	77	58	52	27	43	27	59	55	126	83	317	350	219	101	95	27	24	1794
Friday	9	7	1	0	6	0	46	77	92	42	56	79	46	128	52	102	31	384	230	163	92	44	0	64	1751
Saturday	6	34	22	4	1	3	16	74	99	82	46	86	70	93	92	271	162	604	305	295	82	47	16	43	2555
Sunday	24	9	3	0	0	0	1	15	47	16	83	56	80	79	157	19	67	47	74	12	30	3	44	37	905
Sum	56	76	33	4	13	25	135	458	458	294	391	377	412	574	655	753	574	1905	1409	974	531	276	154	205	10743

(b) Trespassing Pedestrians

Day/Time	0:00	1:00	2:00	3:00	4:00	5:00	6:00	7:00	8:00	9:00	10:00	11:00	12:00	13:00	14:00	15:00	16:00	17:00	18:00	19:00	20:00	21:00	22:00	23:00	Sum
Monday	3	1	2	0	0	1	3	7	25	20	41	17	26	43	75	10	28	23	30	6	13	1	11	6	392
Tuesday	1	0	0	0	0	5	11	47	32	28	45	40	63	56	53	82	64	60	39	49	40	13	6	3	737
Wednesday	3	6	0	0	3	2	10	35	53	35	44	31	36	51	58	83	82	110	69	30	40	14	14	5	814
Thursday	5	5	0	0	1	3	15	42	52	38	34	30	20	52	44	85	77	127	91	36	39	16	15	11	838
Friday	1	5	1	0	2	0	25	39	39	30	31	32	30	49	26	82	28	133	66	33	25	13	0	11	701
Saturday	6	13	7	1	3	3	7	70	65	30	31	51	75	52	49	94	97	171	82	77	28	16	8	6	1042
Sunday	6	2	0	0	0	0	6	17	43	16	53	14	41	32	97	14	51	11	59	2	11	0	18	16	509
Sum	25	32	10	1	9	14	77	257	309	197	279	215	291	335	402	450	427	635	436	233	196	73	72	58	5033

(c) Trespassing Vehicles

Fig. 12. Trespass Distribution by Time and Day (a) Events; (b) Pedestrians; and (c) Vehicles.

- In terms of hour of the day, 5PM – 6PM had the largest proportion of trespassing events (12%), trespassing pedestrians (18%), and trespassing vehicles (13%). For a broader time, a majority of trespassing events occurred between 3PM and 7PM, involving larger numbers of trespassing vehicles and pedestrians. This trend is consistent with a previous study, in which the FRA (2018a) investigated the percentage of trespass fatalities and concluded that the highest percentage of trespass fatalities occur in the evening commute hours, between 4:00 pm and 8:00 pm (23%). In this case study, one hypothesis is that in the timeframe from 4 PM to 7 PM, many commuters are making their way back to their homes by train. Since two major parking lots are located on the west side of the rail track and New York-bound trains also move on the west track of this double-track line, most commuters can take the train from the same side in the morning rush hour and do not need to walk through intersections. On the other hand, during evening commute hours, most people arrive at the train station and needed to walk through this grade crossing to get to the parking lots.

- In terms of day of the week, Saturday has the greatest number of trespassing events (21%), trespassing pedestrians (24%), and trespassing vehicles (21%). Similar conclusion was also drawn in the previous studies regarding trespassing accidents resulting in fatalities. The FRA (2018b) stated that Saturday accounts for the highest percentage of trespass fatalities (17%) and the trespass distribution may not strictly follow common work and commuting schedules.

The overall trend of trespassing vehicles is identical to trends of trespassing events in general. It indicates that the number of trespassing vehicles per violation event has insignificant variations. In terms of trespassing pedestrians per event, each trespassing event from 5PM to 7PM would involve a larger group of violating pedestrians than any other timestamp. The Kolmogorov–Smirnov (KS) test is employed to validate the similarity of these three distributions. The P-value of trespassing events and trespassing pedestrians is much smaller than 0.05, which indicates that there is a significant difference between these two distributions, while the KS test for trespassing events and trespassing vehicles shows the two have close distributions (P-value = 0.06943).

4.5. *Rates of trespass vehicle*

Fig. 13 illustrates the distribution of the trespassing vehicle rate by hour of the day and day of the week. The trespassing vehicle rate is defined as the number of trespassing vehicles per 1,000 vehicles in this location. For the time of day, each hour within daylight periods (e.g., 7AM-8PM) has a similar trespassing rate for vehicles. This indicates that although evening time has rush hour traffic and greater trespassing frequency, the trespassing vehicle rate per unit traffic volume (1,000 vehicles) does not have significant variations. Overall, the daylight periods (e.g., from 7AM to 8PM) have similar trespass vehicle rate, which are greater than these in night periods. This may result from relatively smaller approaching trains with lower frequency of closing gates.

4.5.1. *Correlation matrix with hourly trespass data*

To ascertain the correlations between multiple variables, the correlation matrix based upon Pearson correlation is computed and visualized to investigate the dependence between variables in this section. Correlation matrix can summarize a large amount of data and check patterns explicitly. Pearson correlation coefficient (r), measuring a linear dependence between two variables (X and Y), is one commonly used correlation metric in quantitative variables. It's also known as a parametric correlation test because it depends on the distribution of the data. The Pearson correlation method results in a value in the range [-1, 1].

$$r = \frac{E[(X-\overline{x})(Y-\overline{y})]}{\sigma_X\sigma_Y} = \frac{\sum_{i=1}^{n}(x_i-\overline{x})(y_i-\overline{y})}{\sqrt{\sum_{i=1}^{n}(x_i-\overline{x})^2}\sqrt{\sum_{i=1}^{n}(y_i-\overline{y})^2}} \tag{6}$$

Where:X and Y are two variables$n$ is population sizex_i and y_i are the individual points indexed with $i\overline{x}$ and $\overline{y}$ are the mean values of two variables (X and Y)σ_X and σ_Y are the standard deviation of two variables (X and Y)

In general, the value of the correlation coefficient can vary between −1 and 1. −1 indicates a strong negative correlation: every time × increases, y decreases. 0 means that there is no association between the two variables (x and y). 1 indicates a strong positive correlation: y increases with x. Meanwhile, Pearson correlation isn't defined when the data is categorical. One common option is to use one-hot encoding to break each possible option of each categorical feature to 0-or-1 features. In this case, one-hot encoding is applied to two potentially significant variables, which are daylight period and weather conditions. Nine (9) collected fields are processed and each record represents trespass statistics (e.g., trespassing frequency, trespassing vehicles, and trespassing pedestrians), train and highway traffic (e.g., vehicle traffic, train frequency), and environment conditions (e.g., weather, daylight period) based on a one-hour period. Table 3 demonstrates the basic statistics of these variables.

Fig. 14 presents a graphical display of developed correlation matrix and highlights the most correlated variables with red coefficients in the data table. In this plot (Fig. 14), It is rational that trespassing frequency and number of trespassing pedestrians in one hour have significant positive correlations with each other. Take trespassing frequency, trespassing vehicles, and trespassing pedestrians as three objective variables, hourly vehicle count has large correlation coefficients with objective variables (around 0.5). It indicates that hourly traffic volumes have the most positive correlation with trespassing frequency, number of trespassing vehicles and pedestrians. More vehicle traffic and greater trespass frequency takes place in this grade crossing. Instead, the number of passing trains in one hour has relatively lower correlations (0.34, 0.32, and 0.33) with three trespassing objective variables comparing to roadway traffic. In a 24-hour cycle, night and day have slightly negative and positive correlations, respectively, with objective variables. Weather conditions as clear and cloudy also have positive Pearson correlation with objective variables. Weather conditions in fog, rain, or snow and ratio of trespassing after train have the smallest Pearson correlation values. It is also acknowledged that small sample sizes (e.g., number of trespasses in fog or snow) may affect the development of correlations with trespass counts.

4.6. *Discussions and recommendations*

For a case study of one grade crossing in New Jersey, the developed AI-aided automated trespassing detection technology has processed two months and one week of raw video data efficiently and with acceptable level of accuracy. On average, there are around 45 unsafe trespassing acts occurring daily in this location, which sees over 100 train passes every day. The analysis of these 3,004 trespassing events presents the distribution of key factors, such as gender, hour of the day, day of the week, violation type, before or after train passes, as well as their correlations. The results presented in this paper are consistent with previous studies, and with newly identified trends in this location-specific case. In addition to highway-rail grade crossing trespassing detection, the developed AI-aided tool can also detect trespasses at rights-of-way without red signal identification as a prerequisite.

While there are a limited number of false positives in the application of the AI-aided detection tool, the collected trespassing events and

Day/Time	0:00	1:00	2:00	3:00	4:00	5:00	6:00	7:00	8:00	9:00	10:00	11:00	12:00	13:00	14:00	15:00	16:00	17:00	18:00	19:00	20:00	21:00	22:00	23:00	Sum
Monday	7	2	2	0	0	2	7	12	23	19	26	9	14	24	36	5	13	9	14	3	10	1	16	13	13
Tuesday	3	0	0	0	0	7	11	36	20	19	28	21	35	31	28	32	25	19	16	26	32	12	10	9	23
Wednesday	9	15	0	0	6	3	13	36	44	26	31	20	23	31	35	37	34	37	30	17	31	12	21	14	27
Thursday	8	12	0	0	4	4	14	28	29	24	22	18	11	30	25	41	35	37	33	17	28	11	17	20	25
Friday	2	10	3	0	14	0	20	27	24	20	21	21	18	32	16	34	11	41	26	16	18	10	0	19	21
Saturday	10	20	10	3	10	4	5	41	34	17	17	28	42	29	25	32	35	50	30	33	17	10	8	8	27
Sunday	8	3	0	0	0	0	7	11	28	9	32	7	20	16	41	6	21	4	22	1	8	0	19	23	14
Sum	7	9	3	0	4	3	11	28	29	19	25	18	23	27	30	27	25	29	25	16	20	8	13	16	22

Fig. 13. Distribution of Trespass Vehicle Rate by Time and Day.

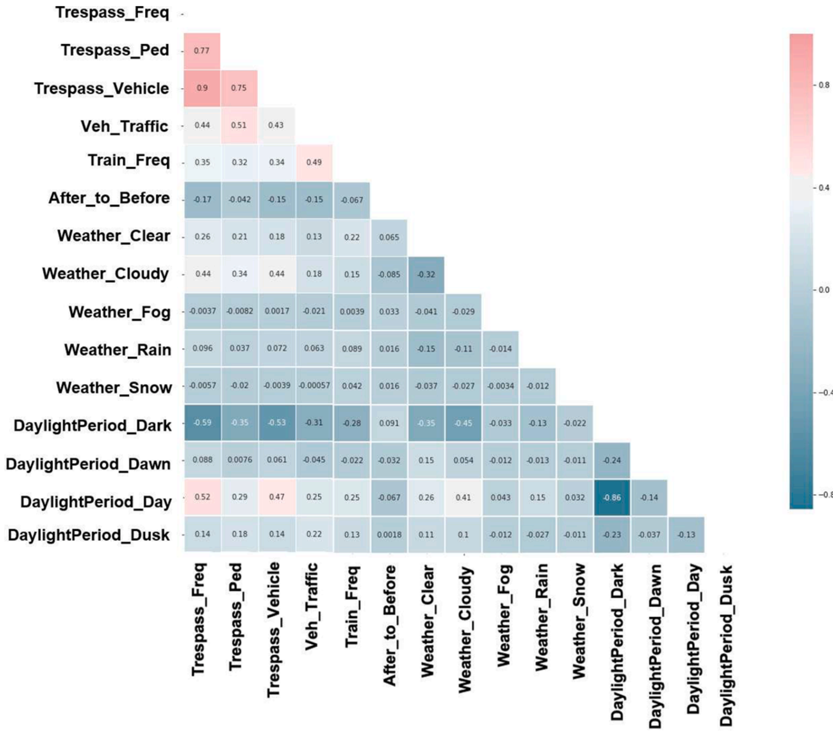

Fig. 14. Pearson Correlation Matrix of Recorded Trespassing Events in Hourly Data.

preliminary analysis can be informative for proactive safety actions in engineering, education, and law enforcement (3 E's) and could even save lives. The statistical value of a life at over $9 million, a value employed by the railroad industry (FRA, 2016b), justifies the significance of such safety practices. Below are three trespassing mitigation strategies per the analysis of the collected trespassing events.

4.7. Law enforcement at peak trespassing hours

To reduce the number of trespassers in this location through law enforcement, it is recommended to post police officers at the railroad crossing during peak trespassing hours. Having police officers at the crossing can deter pedestrians and vehicles from trespassing. According to previous explanatory analyses, most trespasses occurred from 3PM to 7PM on Thursday and Saturday (24% of trespassing pedestrians and 17% of trespassing vehicles for the whole week). Specifically, these 8 labor hours of a police officer per week could put 177 pedestrians and 89 vehicles expected to be trespassers within view of law enforcement, and most of them would be anticipated to behave compliantly under these conditions. Considering that more trespasses occur during warm and clear weather, more law enforcement could be placed at the grade crossing during summer and/or clear days. With an increased budget, law enforcement could be present from 3PM – 7PM for the whole week, which would account for and possibly prevent around half of all trespassing pedestrians and trespassing vehicles.

4.8. Engineering with pedestrian channelization

At this location, some pedestrians can go around or under the gates and 217 trespasses were also observed with fully closed gates (horizontal gates). This population is particularly worrisome as they are the most probable trespassers to be struck by a train. The usage of a swing gate at the four corners would prohibit pedestrians from crossing in an unsafe way and provide a set route for them to follow (Fig. 15). When the red signal comes on, the gates will lock from the outside of the tracks so that people cannot enter. The gates will also have a push-bar on the inside (track side) that will allow pedestrians who are already on the tracks when the red signal activates to exit at all times. This will also force pedestrians to look at the tracks before they cross to ensure it is safe. An example of a swing gate is shown below. The FRA (2008)

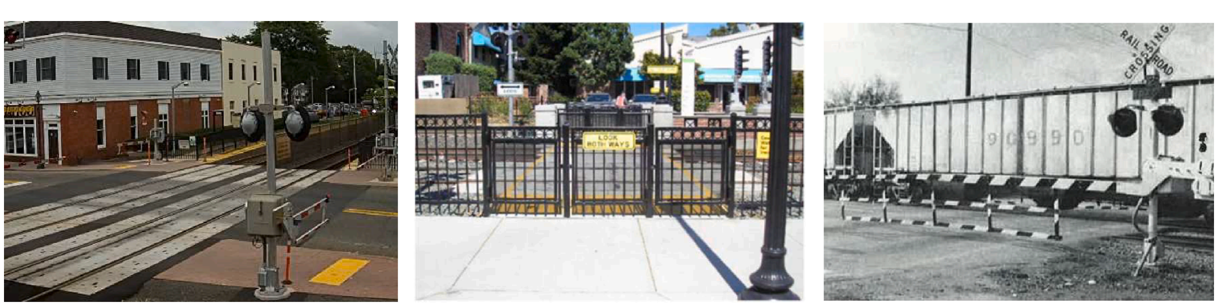

(a) (b) (c)

Fig. 15. Gate Options (a) Prototype Gate at the Selected Location; (b) Swing Gate in California; and (c) Gate Arm and Skirt at Knoxville, TN. Notes: Images: (b) California Public Utilities Commission, Pedestrian-Rail Crossings in California (c) Chase et al., 2013.

concluded that the use of swing gates in Salt Lake City's light rail system has reduced incidents related to passenger inattention to trains around transit stations. However, it is acknowledged that swing gates are more beneficial in pedestrian-only crossings, while in this selected crossing, they cannot absolutely prevent all trespassing pedestrians. Instead, swing gates may result in more trespassing pedestrian violations via the gaps between or under vehicle gates. Thus, installation of longer automatic gate arms and vehicle gate skirts can serve as supplementary solutions. A previous study (Chase et al., 2013) has proven that pedestrian gate skirts can reduce the number of pedestrian violations while the gates are descending and horizontal. Similarly, vehicle gate skirts are expected to prevent pedestrians who avoid existing pedestrian gate skirts and choose to violate by going under vehicle gates. These additional engineering actions can also contribute to the prevention of trespassing pedestrians and even trespassing vehicles.

4.9. Target-specific education

The analysis of collected trespassing events provides clear reference for education among school bus drivers and local authorities, as well as education actions during winter and at local recreational establishments.

- In the studied period, there were several school buses violating the red signals at the grade crossing (Fig. 16a). This is a serious issue since two schools are located near the grade crossing and school buses should regularly travel through it. These noncompliant actions put young students at high risk. Additionally, the violations might have a potentially adverse impact on school students, in particular for the ones regularly riding trespassing buses.
- The trespassing data included a total of thirteen police car violations and one ambulance violation (Fig. 16b and c). It is important to emphasize that incoming trains cannot make positive stops for local authorities, even in the case of local emergencies. It is the police's responsibility to protect the people, however they should not be doing it in a way that puts their own lives at risk. One recent minor accident occurred when a Texas deputy's vehicle was hit by a train while responding to a call (FOX NEWS, 2019). With basic education regarding grade crossing safety, officers can strictly follow the rules, which can help prevent unnecessary accidents and save lives.
- The higher trespassing vehicle rate in August discloses that on average, vehicles traveling through this location have slightly greater likelihood of trespassing in warmer seasons. Thus, more safety education can be delivered in summer to reduce the possibility of driving violation.

(a)

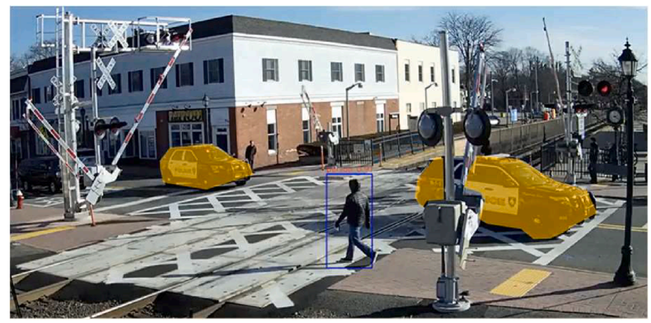

(b)

(c)

Fig. 16. Trespassing with (a) School Bus; (b) Police Cars; and (c) Ambulance. Notes: Authorized emergency vehicles (e.g., police car and ambulance) are manually masked.

5. Conclusions

This paper presents a state-of-the-art AI-aided methodology with high-accuracy fast-processing railroad trespassing detection capabilities for both highway-rail grade crossings and rights-of-way. The applications of YOLO and computer vision in trespassing detection have been validated in around 1,632 h of videos with reasonable accuracy. Around 3,000 trespassing violations are detected and recorded during the analyzed period. In the location-specific case study, the collected trespassing database discloses that most trespassing events occurred from 4PM to 7PM, on Saturday out of all days of the week, and after train passing. In particular, 1AM-2AM on Saturday has the largest trespass pedestrian rate. Although the number of males and females are identical in local area, male trespassers are twice as likely to trespass as their female counterparts. Additionally, the correlation matrix demonstrates that vehicle traffic and pedestrian count have significant correlations with trespassing frequency and numbers of trespassing violators (e.g., vehicles, pedestrians). Accordingly, potential mitigation solutions are proposed from engineering, enforcement, and education perspectives. Overall, this AI-based trespassing detection can contribute to harnessing the potential of big video data to obtain a better understanding of real-world trespassing behaviors and characteristics with the collection of near-miss events. The development of informed risk-mitigation strategies can enhance the safety of the train crew, rail passengers, and road users and aid in the relief of congestion by reducing the number of accidents and incidents.

6. Future work

Firstly, future work would focus on accuracy improvement by mitigating noise from sunlight on the surface of red signal and extreme weather conditions. For example, the automatic identification of grade crossings gate position can be used as a supplemental activation trigger. Moreover, analyses of passive, non-signalized grade crossings can also be explored in the future. Secondly, future work can investigate the possibility of integrating a proposed AI-based trespassing detection tool with Positive Train Control (PTC) systems and highway Intelligent Transportation Systems (ITS). Although preventing grade-crossing accidents is not specifically addressed in the PTC mandate, one prior study (CRS, 2018) pointed out that this could be achieved technically within the PTC framework by installing sensors at crossings that would engage the brakes of an oncoming train if a crossing gate is not working properly or if a vehicle is detected on the tracks. More research is needed for grade-crossings and rights-of-way safety improvement in the age of PTC systems.

CRediT authorship contribution statement

Zhipeng Zhang: Methodology, Validation, Formal analysis, Investigation, Data curation, Writing – original draft. **Asim Zaman:** Validation, Investigation, Data curation. **Jinxuan Xu:** Conceptualization, Methodology, Supervision, Writing – original draft, Project administration. **Xiang Liu:** Investigation, Methodology, Project administration, Writing – review & editing.

Declaration of Competing Interest

The authors declare that they have no known competing financial interests or personal relationships that could have appeared to influence the work reported in this paper.

Acknowledgements

The authors thank Mr. Francesco Bedini Jacobini from the FRA, Mr. Marco daSilva from the Volpe National Transportation Systems Center, and Mr. Todd Hirt from the NJDOT for their feedback and insight during this research. The first author was financially supported by the Rutgers, The State University of New Jersey in the preparation of this manuscript. The views and opinions expressed herein at these of the authors.

References

Arabi, S., Haghighat, A., Sharma, A., 2020. A deep-learning-based computer vision solution for construction vehicle detection. Comput.-Aided Civ. Infrastruct. Eng. 35 (7), 753–767.

Catalano, A., Bruno, F.A., Pisco, M., Cutolo, A., Cusano, A., 2014. In: May. Intrusion detection system for the protection of railway assets by using fiber Bragg grating sensors: a case study. IEEE, pp. 1–3.

Chadwick, S.G., Zhou, N., Saat, M.R., 2014. Highway-rail grade crossing safety challenges for shared operations of high-speed passenger and heavy freight rail in the US. Saf. Sci. 68, 128–137.

Chakraborty, P., Adu-Gyamfi, Y.O., Poddar, S., Ahsani, V., Sharma, A., Sarkar, S., 2018. Traffic congestion detection from camera images using deep convolution neural networks. Transp. Res. Rec. 2672 (45), 222–231.

Chase, S.G., Gabree, S.H., DaSilva, M., 2013. Effect of Gate Skirts on Pedestrian Behavior at Highway-Rail Grade Crossings. DOT/FRA/ORD-13/51, Washington DC.

Congressional Research Service (CRS), 2018. Positive train control (PTC): overview and policy issues. R42637, Washington DC.

DaSilva, M.P., Baron, W. and Carroll, A.A., 2012. Highway rail-grade crossing safety research: Railroad infrastructure trespassing detection systems research in Pittsford, New York (No. DOT-VNTSC-FRA-05-07).

Dee, H.M., Velastin, S.A., 2008. How Close Are We to Solving the Problem of Automated Visual Surveillance? Mach. Vision Application 19 (5-6), 329–343.

Elias, B., Peterman, D.R., Frittelli, J., 2016. Transportation security: issues for the 114th congress. Library of Congress, Congressional Research Service 7–5700. May 9, 2016.

Federal Railroad Administration, 2008. Compilation of pedestrian safety devices in use at grade crossings. Washington DC.

Federal Railroad Administration, 2015. The Fixing America's Surface Transportation Act (P.L. 114-94).

Federal Railroad Administration, 2016a. Highway-rail grade crossing & trespassing. Fact Sheet, Washington DC.

Federal Railroad Administration, 2016b. Benefit-cost analysis guidance for rail projects, U.S. Dept. of Transportation, Washington, DC.

Federal Railroad Administration, 2018a. Railroad Crossing Safety and Trespass Prevention. https://www.fra.dot.gov/Media/File/1199, Washington DC.

Federal Railroad Administration, 2018b. National Strategy to Prevent Trespassing on Railroad Property. Report to Congress, October 2018. Washington DC.

FOX NEWS, 2019. Texas deputy's vehicle hit by train as he rushed to save baby in distress, officials say. https://www.foxnews.com/us/texas-deputy-vehicle-train-baby-distress,.

Federal Railroad Administration, 2019a. A Literature Review of Rail Trespassing and Suicide Prevention Research. TRB's Transportation Research Circular E-C242.

Federal Railroad Administration., 2019b. Highway-Rail Grade Crossing Accident/Incident (6180.57) Database. https://safetydata.fra.dot.gov/OfficeofSafety/publicsite/on_the_fly_download.aspx. (Accessed in August, 2019).

Frittelli, J., 2018. Trespassing: The Leading Cause of Rail-Related Fatalities No. IN10753.

George, B.F., 2008. Rail Trespasser Fatalities Demographic and Behavioral Profiles [Online] (Accessed 07-12 2015), Available from: Cadle Creek Consulting. https://www.fra.dot.gov/eLib/Details/L02669.

Girshick, R., Donahue, J., Darrell, T., Malik, J., 2014. Rich feature hierarchies for accurate object detection and semantic segmentation. In: Proceedings of the IEEE Conference on Computer Vision and Pattern Recognition, pp. 580–587.

Havârneanu, G.M., Burkhardt, J.-M., Paran, F., 2015. A systematic review of the literature on safety measures to prevent railway suicides and trespassing accidents. Accid. Anal. Prev. 81, 30–50.

Kalman, R.E., 1960. A new approach to linear filtering and prediction problems. J. Basic Eng. 82 (1), 35–45.

Laroca, R., Severo, E., Zanlorensi, L.A., Oliveira, L.S., Gonçalves, G.R., Schwartz, W.R., Menotti, D., 2018. In: July. A robust real-time automatic license plate recognition based on the YOLO detector. IEEE, pp. 1–10.

Le, N., Heili, A., Odobez, J.M., 2016. In: October. Long-term time-sensitive costs for CRF-based tracking by detection. Springer, Cham, pp. 43–51.

Lin TY. et al. Microsoft COCO: Common Objects in Context. Computer Vision – ECCV 2014. Zurich, 2014. pp. 740-755 https://doi.org/10.1007/978-3-319-10602-1_48.

Lobb, B., Harré, N., Terry, N., 2003. An evaluation of four types of railway pedestrian crossing safety intervention. Accid. Anal. Prev. 35 (4), 487–494.

Ngamdung, T., 2019. Effect of Grade Separation on Pedestrian Railroad Trespass Activity at Shuttlesworth Drive in Collegeville, AL. Federal Railroad Administration, DOT/FRA/ORD-19/11. May 2019.

Qu, T., Zhang, Q., Sun, S., 2017. Vehicle detection from high-resolution aerial images using spatial pyramid pooling-based deep convolutional neural networks. Multimedia Tools and Applications 76 (20), 21651–21663.

Poulos, R.G., Hatfield, J., Rissel, C., Flack, L.K., Shaw, L., Grzebieta, R., McIntosh, A.S., 2017. Near miss experiences of transport and recreational cyclists in New South Wales, Australia. Findings from a prospective cohort study. Accid. Anal. Prev. 101, 143–153.

Redmon, J., Divvala, S., Girshick, R., Farhadi, A., 2016. You only look once: Unified, real-time object detection. In: In Proceedings of the IEEE Conference on Computer Vision and Pattern Recognition, pp. 779–788.

Redmon, J. and Farhadi, A., 2018. YOLOv3: An incremental improvement. arXiv preprint arXiv:1804.02767.

Rosenbloom, T., Haviv, M., Peleg, A., Nemrodov, D., 2008. The effectiveness of road-safety crossing guards: Knowledge and behavioral intentions. Saf. Sci. 46 (10), 1450–1458.

Savage, I., 2016. Analysis of fatal train-pedestrian collisions in metropolitan Chicago 2004–2012. Accid. Anal. Prev. 86, 217–228.

Silla, A., Luoma, J., 2012. Main characteristics of train-pedestrian fatalities on Finnish railroads. Accid. Anal. Prev. 45, 61–66.

Stanchak, K. and DaSilva M., 2014. Trespass Event Risk Factors. Federal Railroad Administration, DOT/FRA/ORD-14/32. Washington DC.

Taylor, J.A., Lacovara, A.V., Smith, G.S., Pandian, R., Lehto, M., 2014. Near-miss narratives from the fire service: a Bayesian analysis. Accid. Anal. Prev. 62, 119–129.

Topel, K., 2019. A Literature Review of Rail Trespassing and Suicide Prevention Research. Transportation Research Circular (E-C242).

U.S. Census Bureau, 2019. Bergen County, New Jersey Gender Ratios. Accessed by May 13, 2019.

Volpe The National Transportation Systems Center, 2015. Trespassing Detection and Warning Research, Brunswick, ME. 2015 ROW fatality & Trespass Prevention Workshop, Charlotte, NC.

Wright, L., van der Schaaf, T., 2004. Accident versus near miss causation: a critical review of the literature, an empirical test in the UK railway domain, and their implications for other sectors. J. Hazard. Mater. 111 (1-3), 105–110.

Yencha, C., 2019. Valuing walkability: New evidence from computer vision methods. Transp. Res. Part A: Policy Pract. 130, 689–709.

Zaman, A., Ren, B., Liu, X., 2019. Artificial Intelligence-Aided Automated Detection of Railroad Trespassing. Transp. Res. Rec. 2673 (7), 25–37.

Zhang, J., Huang, M., Jin, X., Li, X., 2017. A real-time Chinese traffic sign detection algorithm based on modified YOLOv2. Algorithms 10 (4), 127.

Zhang, M., Khattak, A.J., Liu, J., Clarke, D., 2018a. A comparative study of rail-pedestrian trespassing crash injury severity between highway-rail grade crossings and non-crossings. Accid. Anal. Prev. 117, 427–438.

Zhang, Z., Trivedi, C., Liu, X., 2018b. Automated detection of grade-crossing-trespassing near misses based on computer vision analysis of surveillance video data. Saf. Sci. 110, 276–285.